

Published in final edited form as:

*J Med Chem.* 2011 May 12; 54(9): 3306–3318. doi:10.1021/jm101651b.

## Potent Bivalent Smac Mimetics: Effect of the Linker on Binding to Inhibitor of Apoptosis Proteins (IAPs) and Anticancer Activity

Haiying Sun<sup>+</sup>, Liu Liu<sup>+</sup>, Jianfeng Lu<sup>+</sup>, Longchuan Bai<sup>+</sup>, Xiaoqin Li<sup>Δ</sup>, Zaneta Nikolovska-Coleska<sup>+</sup>, Donna McEachern<sup>+</sup>, Chao-Yie Yang<sup>+</sup>, Su Qiu<sup>+</sup>, Han Yi<sup>+</sup>, Duxin Sun<sup>Δ</sup>, and Shaomeng Wang<sup>\*</sup>

<sup>+</sup> Comprehensive Cancer Center and Departments of Internal Medicine, Pharmacology and Medicinal Chemistry, University of Michigan, Ann Arbor, MI 48109, USA

<sup>Δ</sup> Department of Pharmaceutical Sciences, College of Pharmacy, University of Michigan, Ann Arbor, MI 48109, USA

### Abstract

We have synthesized and evaluated a series of non-peptidic, bivalent Smac mimetics as antagonists of the inhibitor of apoptosis proteins and new anticancer agents. All these bivalent Smac mimetics bind to full-length XIAP with low nanomolar affinities and function as ultra-potent antagonists of XIAP. While these Smac mimetics bind to cIAP1/2 with similar low nanomolar affinities, their potencies to induce degradation of cIAP1/2 proteins in cells differ by more than 100-fold. The most potent bivalent Smac mimetics inhibit cell growth with IC<sub>50</sub> values from 1–3 nM in the MDA-MB-231 breast cancer cell line and are 100-times more potent than the least potent compounds. Determination of intracellular concentrations for several representative compounds showed that the linkers in these bivalent Smac mimetics significantly affect their intracellular concentrations, hence the overall cellular activity. Compound **27** completely inhibits tumor growth in the MDA-MB-231 xenografts, while causing no signs of toxicity in the animals.

### Introduction

Apoptosis is a critical cell suicide process by which damaged or unwanted cells are removed. It plays an important role in homeostasis, normal development, host defense and suppression of oncogenesis. Dysfunction of apoptosis machinery is a hallmark of cancer<sup>1</sup> and defects in the apoptosis machinery confer on cancer cells resistance to current anticancer therapies, making them less effective and leading to their ultimate failure.<sup>2</sup> Targeting key apoptosis regulators with the goal of promoting apoptosis in tumor cells is therefore being pursued as a new therapeutic strategy for human cancer.<sup>3</sup>

The inhibitor of apoptosis proteins (IAPs) are a class of key apoptosis regulators and are characterized by the presence of one or more baculoviral IAP repeat (BIR) domains.<sup>4–7</sup> Among a total of 8 mammalian IAPs, X-linked IAP (XIAP) inhibits apoptosis by directly binding to and effectively inhibiting three caspases, caspase-3, -7, and -9.<sup>4–7</sup> The third BIR domain (BIR3) of XIAP binds to the processed caspase-9 and inhibits its activity, and the BIR2 domain of XIAP, together with the linker preceding it, binds to and inhibits both caspase-3 and caspase-7. Hence, XIAP plays a central role in the inhibition of apoptosis by inhibiting these three caspases. Two other IAPs, cIAP1 and cIAP2 were originally identified through their interaction with tumor necrosis factor associated factor 2 (TRAF2).<sup>4</sup> This interaction leads to their recruitment to TNF receptor 1- and 2-associated complexes, where

<sup>\*</sup>To whom correspondence should be addressed. Phone: (734)615-0362. Fax: (734)6479647. shaomeng@umich.edu.

they suppress caspase-8 activation and death-receptor-mediated apoptosis.<sup>4</sup> Furthermore, although these IAPs were initially characterized for their role in apoptosis regulation, they also modulate many other cellular processes, such as inflammation, proliferation, mitosis and metastasis,<sup>8–10</sup> which are frequently deregulated in cancer and contribute directly or indirectly to tumor initiation, maintenance and/or progression. Accordingly, these IAP proteins are very attractive cancer therapeutic targets.<sup>11–13</sup>

The second mitochondria derived activator of caspases (Smac) or direct IAP binding protein with low pI (DIABLO) has been identified as an endogenous antagonist of IAP proteins.<sup>14,15</sup> Once released from mitochondria into the cytosol, Smac is processed by proteases to remove the first 55 N-terminal residues, exposing an Ala-Val-Pro-Ile (AVPI) tetrapeptide binding motif.<sup>14,15</sup> Smac forms a homodimer and promotes apoptosis by directly interacting with and antagonizing XIAP and cIAP1 and cIAP2.<sup>7</sup> In its homodimer form, Smac protein binds concurrently to both the BIR2 and BIR3 domains of XIAP using two AVPI binding motifs and nullifies the inhibition of XIAP to caspase-9 and caspase-3/7.<sup>7</sup> Smac binds to the BIR3 domain, but not to other BIR domains of cIAP1 and cIAP2, *via* a single AVPI binding motif.<sup>19</sup> By antagonizing these multiple IAP proteins, Smac efficiently promotes apoptosis. There have been intense research efforts in recent years in the design and development of small-molecule Smac mimetics as a new class of anticancer drugs.<sup>20–35</sup> Two different types of Smac mimetics have been designed; monovalent Smac mimetics possess one AVPI mimic and bivalent Smac mimetics contain two AVPI mimics tethered with a linker.<sup>20,21</sup> Representatives of previously reported monovalent and bivalent Smac mimetics are shown in Figure 1 and Figure 2, respectively.

Although Smac mimetics were initially designed primarily based upon the interaction between Smac and XIAP proteins, recent studies have shown that Smac mimetics induce rapid degradation of cIAP proteins in cells.<sup>36–39</sup> One major difference between bivalent and monovalent Smac mimetics is their ability to antagonize XIAP. While monovalent Smac mimetics can potentially antagonize the inhibition of XIAP BIR3 protein to the activity of caspase 9, they are much less effective in antagonizing the inhibition of caspase-9 and 3 by XIAP protein containing both BIR2 and BIR3 domains.<sup>39</sup> In comparison, bivalent Smac mimetics function as ultra-potent antagonists of XIAP protein containing both BIR2 and BIR3 domains through currently binding to both BIR domains.<sup>28,39</sup> Both monovalent and bivalent Smac mimetics are effective in killing cancer cells in a subset of human cancer cell lines in a TNF $\alpha$ -dependent manner,<sup>36–39</sup> but bivalent Smac mimetics are much more potent than their corresponding monovalent Smac mimetic analogues.<sup>39</sup> One major advantage for monovalent Smac mimetics, however, is their much favorable pharmacokinetic properties; properly designed monovalent Smac mimetics can achieve excellent oral bioavailability.<sup>20,21</sup> To date, three monovalent Smac mimetics and two bivalent Smac mimetics have been advanced into early clinical development for cancer treatment.<sup>20</sup> Of which, an orally active monovalent Smac mimetic, SM-406/AT-406 (compound **9** in Figure 1) from our group, is currently in Phase I clinical trials.<sup>23</sup> The chemical structures of the other four clinical stage compounds have not been disclosed.

Starting from a non-peptide, monovalent Smac mimetic, **15**, we have designed and synthesized a bivalent Smac mimetic **16** (Figure 3).<sup>35,39</sup> We have shown that **16** is >100-times more potent in binding to XIAP containing both BIR2 and BIR3 domains, and 10-times more potent in binding to cIAP1 BIR3 protein and cIAP2 BIR3 protein, than **15**.<sup>35,39</sup> Compound **16** is capable of effectively inducing apoptosis and inhibiting cell growth in a subset of human cancer cell lines at concentrations as low as 1–10 nM and is 100-times more potent than **15**.<sup>39</sup> Furthermore, **16** also strongly induces apoptosis in MDA-MB-231 xenograft tumor tissues and achieves tumor regression at 5 mg/kg in the MDA-MB-231 xenograft model in mice.<sup>39</sup> These *in vitro* and *in vivo* data identify compound **16** as a

promising lead for further structure-activity relationship studies, with the ultimate goal of developing a potent bivalent Smac mimetic for the treatment of human cancer.

We report here the design, synthesis and evaluation of a series of analogues of **16**, as well as several control compounds (Figure 4). One main objective in the present study was to investigate the effect of the linker on binding affinities to XIAP and cIAP1/2 proteins and their anticancer activity. Our study has led to the identification of several highly potent bivalent Smac mimetics and yielded new structure-activity insights into the design of potent bivalent Smac mimetics as a new class of anticancer drugs.

## Chemistry

The synthesis of the newly designed compounds **18–30** is similar to that of **16** and is shown in Scheme 1.<sup>35</sup> Briefly, the key intermediate **31** was synthesized using a method we published previously.<sup>35</sup> Cycloaddition of **31** with corresponding bis-azide in the presence of CuSO<sub>4</sub> and (+)-sodium-*L*-ascorbate afforded a series of bis-triazoles, removal of the Boc protecting groups, which gave compounds **18–29**. Cycloaddition of **31** with excess 1,4-bis-4-azidobutylbenzene, catalyzed by CuSO<sub>4</sub> and (+)-sodium-*L*-ascorbate, furnished **32**, which was reacted with **33** to afford a bis-triazole.<sup>35</sup> Removal of the Boc protecting group from this bis-triazole gave **30**.

## Results and Discussion

Compound **16** is a bivalent Smac mimetic containing two monovalent IAP binding motifs, tethered together through a flexible linker.

In order to explore the influence of the linker region on the activity of bivalent Smac mimetics, we designed a series of new analogues (compounds **18–29** in Figure 4) with linkers of various lengths, flexibility and hydrophobicity. A previously synthesized compound (**17**), in which both *N*-methylalanine residues were replaced with *N*-acetyltryptophan groups, and compound **30**, in which one *N*-methylalanine residue in **16** has been replaced with *N*-acetyltryptophan, were employed as control compounds. Compounds **15–30** were tested in fluorescence-polarization (FP) based binding assays for their binding affinities to XIAP, cIAP1 and cIAP2 and the results are summarized in Table 1.

We had shown previously that **16** binds to XIAP BIR3 protein and XIAP protein containing both BIR2-BIR3 domains with different affinities.<sup>35</sup> To evaluate the affinities to XIAP we employed two recombinant XIAP proteins: XIAP BIR3 protein (residues 241–356), which possesses only the BIR3 domain of XIAP, and XIAP L-BIR2-BIR3 (residues 120–356) which contains both BIR2 and BIR3 domains of XIAP and the linker preceding BIR2. Compounds **18–22**, which differ from **16** only in the length of the linker, bind to XIAP L-BIR2-BIR3 protein with very high affinities, achieving IC<sub>50</sub> values of 6–17 nM with calculated K<sub>i</sub> values of 1.5–5.0 nM. These compounds also bind to XIAP BIR3 protein with high affinities and have IC<sub>50</sub> values of 177–613 nM with calculated K<sub>i</sub> values = 55–185 nM. Comparison of their K<sub>i</sub> values for their binding to these two XIAP proteins showed that each of these bivalent Smac mimetics binds to XIAP L-BIR2-BIR3 with an affinity 20–40 times higher than to XIAP BIR3. Notwithstanding the significant differences in the linker lengths in these compounds, the most potent compounds, **16** and **21**, are only three times more potent than the least potent compound (**22**) in their binding affinities to XIAP L-BIR2-BIR3 protein. Our previous study<sup>35</sup> showed that **16** has a higher affinity for XIAP L-BIR2-BIR3 protein than for XIAP BIR3 protein because it concurrently targets both the BIR2 and BIR3 domains. Hence, the binding data for these new analogues to the two XIAP protein constructs also suggest that they concurrently interact with both BIR2 and BIR3 domains in XIAP in the presence of the XIAP protein containing both BIR domains.

We also employed two cIAP1 proteins containing BIR3-only domain or both BIR2 and BIR3 domains to determine if these bivalent Smac mimetics can interact concurrently with both BIR2 and BIR3 domains in cIAP1. Bivalent Smac mimetics **16** and **18–22** bind to cIAP1 BIR3 and cIAP1 BIR2-BIR3 proteins with similar high affinities and have  $K_i = 1–3$  nM to both cIAP1 protein constructs (Table 1). We conclude that in contrast to XIAP, only the BIR3 domain in cIAP1 is involved in the binding to these bivalent Smac mimetics. Compounds **16** and **18–22** also bind to cIAP2 BIR3 protein with very high affinities and have  $K_i = 1–6$  nM. Taken together, these binding data show that these new bivalent Smac mimetics have very high affinities to XIAP and cIAP1/2 proteins and the length of linkers in these bivalent Smac mimetics has only a modest effect on these binding affinities.

We designed **23** and **24**, in which the phenyl group in the linker of **16** is replaced with a more flexible  $(CH_2)_2$  or  $(CH_2)_4$  to investigate the influence of linker rigidity on the binding affinities of bivalent Smac mimetics. Compounds **23** and **24** have potent binding affinities to all of these IAP proteins which are similar to that of **16**, indicating that the rigidity of the linker lacks significant influence on the binding affinities to these IAP proteins.

The linkers in **16–24** are very hydrophobic and in order to explore the influence that polarity and hydrophobicity have on binding affinities to any of these three IAP proteins, we designed compounds **25–29** in which the phenyl group in the linker of **16** is replaced with a more hydrophilic triazole (**25**), urea (**26**), or the entire linker in **16** is replaced with alkyl chains containing one or more oxygen atoms (**27–29**). All of these compounds have binding affinities to these three IAPs similar to that of **16**, indicating that hydrophobicity and polarity in the linker have little influence on the binding affinities.

Finally, focusing on the involvement of the two AVPI mimetics in these bivalent Smac mimetics for binding to XIAP, we designed compound **30**, in which one *N*-methylalanine residue in **16** was replaced with *N*-acetyltryptophan to disrupt the interaction of one AVPI mimetic to these IAP proteins. Compound **30** is 4 times less potent than **16** in binding to XIAP BIR3, but more than 40 times less potent than **16** in binding to XIAP linker-BIR2-BIR3. These data are consistent with our previous study<sup>28</sup> using compound **16** that showed both of the two IAP binding motifs to be involved in the binding to full length XIAP.

These binding data show that in bivalent Smac mimetics, both AVPI motifs are involved in binding to XIAP protein containing both BIR2 and BIR3 domains. The length, conformational rigidity, and hydrophobicity of the linker tethered to the two AVPI mimetics all appear to have only a modest effect on their binding affinities to the XIAP protein containing both BIR2 and BIR3 domains. These data are, however, consistent with the fact that the BIR2 and BIR3 domains in XIAP are connected by a 25-residue segment apparently lacking any significant secondary structure,<sup>40</sup> which would allow XIAP to efficiently interact with bivalent Smac mimetics with linkers of different length, rigidity and hydrophobicity. In comparison, our binding data indicate that only the BIR3 domain in cIAP1 is involved in the binding to these bivalent Smac mimetics.

Because XIAP functions as a potent inhibitor of caspase-9 and caspase-3/-7,<sup>4,7</sup> we evaluated several representative new analogues (**18–22**, **24**, **29** and **30**), together with compounds **15**, **16** and **17**, in cell-free functional assays for their functional antagonism against XIAP (Figure 5). In the caspase-9 functional assay, the XIAP linker-BIR2-BIR3 protein dose-dependently inhibits the activity of caspase-9, achieving 80% inhibition at 500 nM. Bivalent Smac mimetics **16**, **18–21**, **24** and **29** have similar potencies and can restore 60–80% of caspase-9 activity at concentrations of 1.5  $\mu$ M. Interestingly, compound **22** with the longest linker shows much less activity than **16**, restoring only 25% of the caspase-9 activity at 1.5  $\mu$ M concentration. The monovalent Smac mimetic **15** is approximately equipotent with **30**,

in which one side has been disabled, but both compounds are much less potent than **16**, **18–21**, **24** and **29**. The inactive control **17**, at a concentration as high as 100  $\mu\text{M}$ , fails to restore any caspase-9 activity. These results show that both AVPI mimetics in these bivalent Smac mimetics are important to the antagonism of XIAP linker-BIR2-BIR3 proteins in this caspase-9 functional assay.

In the caspase-3/7 functional assay, 20 nM of XIAP protein containing linker-BIR2-BIR3 domains inhibits 90% of the enzymatic activity of caspase-3/7, and bivalent Smac mimetics can dose dependently restore this activity (Figure 6). Most of these bivalent Smac mimetics show activity comparable to that of **16** in this assay. At a 60 nM concentration, the bivalent Smac mimetics **16**, **18–21**, **24** and **29** for example, can restore 55–80% of the activity of caspase-3/7. However, the monovalent compound **15** at 60  $\mu\text{M}$ , at 1,000 times higher concentration, restores only 40% of the caspase-3/7 activity. Compound **30** is only several times less potent than the most potent bivalent Smac mimetics. It is interesting that the inactive control compound **17** shows a comparable potency to **15** in this caspase-3/7 functional assay. Since the BIR2 domain, together with the preceding linker, binds to and inhibits caspase-3/7, such functional data suggest that IAP binding motifs in **17** still can interact with the BIR2 domain of XIAP, although this compound binds to XIAP BIR3 protein with a very low affinity (Table 1). These assay results thus show that bivalent Smac mimetics are highly potent antagonists of XIAP linker-BIR2-BIR3 protein, much more potent than their corresponding monovalent Smac mimetics in both caspase-9 and caspase-3/7 functional assays.

Compound **16** was shown to inhibit cell growth effectively and to induce apoptosis in multiple human cancer cell lines, including the MDA-MB-231 breast cancer cell line.<sup>35,39</sup> Accordingly, the new Smac mimetics were evaluated for their ability to inhibit cell growth in this cell line and the data are summarized in Table 1. It was found that although the linker length in these bivalent Smac mimetics has little influence on the binding affinities to XIAP and cIAP1/2, it has a dramatic effect on the compounds' ability to inhibit cell growth. While the bivalent compound **18**, with the shortest linker, has  $\text{IC}_{50} = 159$  nM and a potency similar to monovalent compound **15**, the analogues with longer linkers in general show cellular activities that increase as the linker length is extended. Compound **21** is the most potent in the series, with  $\text{IC}_{50} = 1.6$  nM, equipotent with **16** and 400 times more potent than **15**. Compound **22** with the longest linker is slightly less potent than **21**, suggesting that the length of the linker in compound **21** is optimal, further extension failing to improve the cellular activity.

The hydrophobicity of the linker also has significant influence on the cellular activity. While **23** and **24** have linkers of length comparable to that of **16** and are as potent as **16** in this cellular assay, compounds **27–29**, which contain one to three oxygen atoms in their linker region, have diminished cellular activity. While **27** has  $\text{IC}_{50} = 19.6$  nM, and is thus 6 times less potent than **16**, **28** has an  $\text{IC}_{50} = 175$  nM, 53 times less potent than **16**. Compound **29**, whose linker contains 3 oxygen atoms, has  $\text{IC}_{50} = 225$  nM, and is 68 times less potent than **16**. Insertion of other polar and hydrophilic groups into the linker also decreases the cellular activity. Compounds **25** and **26**, with a triazole- or a urea-containing linker, have  $\text{IC}_{50} = 107$  and 263 nM respectively in this assay, and thus are 32 and 80 times less potent than **16**. Compound **30** is 203 times less potent than **16** and has the same potency as **15**, indicating the two active IAP binding motifs are required for achieving ultra-potent cellular activity. These data show clearly that the linkers in these bivalent Smac mimetics have a major effect on the compounds' ability to inhibit cell growth.

Previous studies have shown that potent Smac mimetics can induce rapid degradation of both cIAP1 and cIAP2 and that degradation of these cIAP proteins is a prerequisite to

initiation of apoptosis by Smac mimetics in cancer cells.<sup>36–39</sup> To explore the mechanism of action of the bivalent Smac mimetics, we performed western blot analysis of the cIAP proteins in MDA-MB-231 cells treated with compounds **16** and **18–21**. The results are shown in Figure 7. Although these bivalent Smac mimetics bind to cIAP1 and cIAP2 with comparable binding affinities in biochemical assays, they have different potencies in induction of cIAP1/2 degradation, as well as caspase-3 processing and poly(ADP-ribose) polymerase (PARP) cleavage, two biochemical markers of apoptosis. While **19** at 30 nM has little effect on cIAP1 degradation, **20** at a concentration of 10 nM induces clear cIAP1 degradation, whereas the highly potent compounds **16** and **21** induce robust cIAP1 degradation at 1 nM. Similar results have been obtained with respect to their potencies in induction of cIAP2 degradation (Figure 5). At a concentration of 30 nM, both compounds **18** and **19** fail to induce caspase-3 processing and PARP cleavage. In comparison, compound **20** starts to cause PARP cleavage at 3 nM and caspase-3 processing at 10 nM, while compounds **16** and **21** induce robust caspase-3 processing and PARP cleavage at 3 nM concentrations. Thus the western blot analysis shows that the potency of these bivalent Smac mimetics in inhibition of cell growth correlates well with their ability to induce degradation of cIAP1 and cIAP2, PARP cleavage and caspase-3 processing in cancer cells.

Hence, although the linker in the bivalent Smac mimetics has only modest effect on the binding affinities to XIAP and cIAP1/2, it has a significant influence on the cellular activity in inhibition of cell growth, as well as in induction of cIAP1/2 degradation and cleavage of PARP and caspase-3. While the linker determines the distance between the two IAP binding motifs, it also affects the overall hydrophobic properties of a bivalent Smac mimetic. Therefore, we hypothesized that the linker in these bivalent Smac mimetics may have a major effect on their cell permeability and thus the intracellular concentrations of the compounds.

To test this hypothesis, we developed an assay to determine the intracellular concentrations of some representative compounds. In this assay, a compound was incubated with MDA-MB-231 cells at different concentrations for 6 hours or less, *i.e.* before significant cell death occurs. After incubation, the cell culture medium was discarded and the remaining cells were washed promptly and extensively to minimize both the nonspecific adsorption of the compound on outer cell walls and leakage of the compound from the cells during washing. The cells were then lysed and resuspended in water. Concentrations of the compound in the resuspended cell lysates were determined by a sensitive LC-MS/MS technique. Because the exact volume of the cells was unknown, the concentrations of each compound determined in this way are not the actual intracellular concentrations of the compound, but the concentrations of different compounds determined in this way will be a measure of their actual intracellular concentrations.

We evaluated the assay conditions using compounds **16** and **18**, which possess significantly different linker lengths and show different cellular activities, and the results are shown in Figure 8. With a very short incubation time of 15, 30, or 60 seconds, approximately 50 and 10 nM of compounds **16** and **18** were detected in the resuspended cell lysates, but no significant changes were observed for the concentrations of both compounds. The concentrations for both compounds detected with incubation time less than 60 seconds were assumed to represent nonspecific binding, but when the incubation time was extended to one hour, concentrations in cell lysates for compounds **16** and **18** were found to have increased by factors of 5 and 2, respectively, over that observed with incubation time below one minute. Increasing incubation times to 3 and 6 hours did not significantly alter the cell lysate concentrations for both compounds, suggesting that for both compounds, equilibrium between the intra- and extracellular concentrations has been reached after one hour's incubation (Figure 8A). It is also clear that compound **16** has a much higher concentration

than compound **18** in resuspended cell lysates. Compound concentrations obtained were normalized to the total protein amount in the cell lysates to compensate for potentially significant differences in cell numbers in each culture dish. The ratios between these two compounds after normalization (Figure 8B) with incubation times of 1, 3 and 6 hr are consistent with those obtained using concentrations in resuspended cell lysates.

Using these established assay conditions, we next evaluated the intracellular concentrations for three additional representative compounds (**19**, **20** and **29**), together with compounds **16** and **18**. These compounds were incubated with the MDA-MB-231 cells for 1 minute and 3 hours, respectively, and the concentrations in resuspended cell lysates in 100  $\mu$ l of water for each compound were determined using LC-MS/MS. The results are provided in Table 2. After subtraction of the concentration after 1 minute's incubation from that after 3 hr incubation, the concentrations in resuspended cell lysates for these compounds are used to assess their relative intracellular concentrations (Table 2). The data indicated that **16** has the highest intracellular concentration, whereas **29** has the lowest concentration among these compounds. Significantly, the calculated concentrations of these compounds in resuspended cell lysates correlate well with their potencies to induce the degradation of cIAP1/2, as well as their ability to cleave caspase-3 and PARP. These data show that the major difference in the overall cellular activity of these bivalent Smac mimetics, including degradation of cIAP1/2, induction of apoptosis and cell growth inhibition, is most likely due to their different cell permeabilities rather than their different binding affinities to IAP proteins.

We have previously shown that compound **16** was very effective in inhibition of tumor growth in the MDA-MB-231 xenograft model.<sup>39</sup> To further investigate the antitumor activity for this class of compounds, we have evaluated compound **27** for its antitumor activity in the MDA-MB-231 xenograft model based upon its excellent solubility and good *in vitro* activity. The results are shown in Figure 9. Our data showed that **27** inhibits tumor growth in a dose-dependent manner and can completely inhibit tumor growth at 5 mg/kg, while causing minimal weight loss or other signs of toxicity in SCID mice. The antitumor activity is statistically significant ( $p=0.03$  and  $0.0005$  for compound **27** at 1 and 5 mg/kg *versus* the control at the end of the treatment, respectively). The antitumor activity for **27** is also long lasting. On day 50, tumors treated with **27** at 5 mg/kg have an average size of 269  $\text{mm}^3$ , whereas tumors treated with vehicle control have grown to an average size of 1136  $\text{mm}^3$ . In comparison, while taxotere has a similar antitumor activity in this model, it causes significant weight loss during the treatment. Hence, compound **27** is very effective in inhibiting tumor growth of the MDA-MB-231 xenografts at well-tolerated dose-schedules.

## Summary

A series of bivalent Smac mimetics with linkers of various lengths and different hydrophobicities were synthesized and evaluated. These compounds bind to XIAP and cIAP1/2 with very high affinities. They are highly potent XIAP antagonists and efficiently induce cIAP1 and cIAP2 degradation. Several of these new bivalent Smac mimetics, such as compounds **21**, **22** and **24**, are most potent in inhibition of cell growth in the MDA-MB-231 cell line with  $\text{IC}_{50}$  values of 1–3 nM. While the linker has no significant influence on the binding affinities of these bivalent Smac mimetics to XIAP and cIAP1/2, it can dramatically affect their cell permeability, and hence their overall cellular activity. Compound *in vivo* evaluation showed that compound **27** is capable of completely inhibiting tumor growth in the MDA-MB-231 xenograft model. Additional *in vivo* studies are underway with the goal to identify the most promising compounds for advanced preclinical development and the results will be reported in due course.

## Experimental Section

### I. Chemistry

General Methods.  $^1\text{H}$  NMR spectra were acquired at 300 MHz and  $^{13}\text{C}$  spectra at 75 MHz.  $^1\text{H}$  chemical shifts are reported with  $\text{CDCl}_3$  (7.27 ppm) or HDO (4.70 ppm) as internal standards.  $^{13}\text{C}$  chemical shifts are reported relative to  $\text{CDCl}_3$  (77.00 ppm) or 1,4-dioxane (67.16 ppm) as internal standards. The final products were purified by  $\text{C}_{18}$  reverse phase semi-preparative HPLC column with solvent A (0.1% of TFA in  $\text{H}_2\text{O}$ ) and solvent B (0.1% of TFA in  $\text{CH}_3\text{CN}$ ) as eluents. Purity for all the final compounds was determined by reverse phase analytical HPLC to be over 95%.

**Synthesis of bivalent Smac mimetics. General procedure**—A mixture of  $\text{CuSO}_4$  (0.1 eq) and (+)-sodium l-ascorbate (0.3 eq) in  $\text{H}_2\text{O}$  (5 mL per mmol of **31**) was added to a solution of compound **31** (1 eq); then a bis-azide (0.5 eq) in *tert*-butyl alcohol (10 mL per mmol of **31**) was also added. The mixture was stirred at room temperature overnight and then extracted with  $\text{CH}_2\text{Cl}_2$  ( $3 \times 30$  mL). The combined organic layer was washed with brine, dried over  $\text{Na}_2\text{SO}_4$ , and evaporated to afford a residue which was purified by chromatography to give a bis-triazole. HCl (4N in 1,4-dioxane, 2 mL per mmol of bis-triazole) was added to a solution of this bis-triazole in MeOH (5 mL per mmol of bis-triazole). The solution was stirred at room temperature overnight and then concentrated to furnish a crude product which was purified by  $\text{C}_{18}$  reversed phase semipreparative HPLC to give a bivalent Smac mimetic.

**(S,3S,3'S,6S,6'S,10aS,10a'S)-N,N'-((1S,1'S)-(1,1'-(1,4-phenylenebis(methylene))bis(1H-1,2,3-triazole-4,1-diyl))bis(phenylmethylene))bis(6-((S)-2-(methylamino)propanamido)-5-oxodecahydropyrrolo[1,2-a]azocine-3-carboxamide) (18)**—Yield 62% over two steps. Purity was determined by reverse phase analytical HPLC to be over 98%.  $^1\text{H}$  NMR ( $\text{D}_2\text{O}$ ):  $\delta$  7.55 (s, 2H), 7.20-7.02 (m, 10H), 6.82 (brs, 4H), 5.95 (s, 2H), 5.12 (brs, 4H), 4.65 (m, 2H), 4.20 (m, 2H), 4.12 (m, 2H), 3.80 (m, 2H), 2.52 (s, 6H), 2.05-1.15 (m, 30H);  $^{13}\text{C}$  NMR ( $\text{D}_2\text{O}$ ):  $\delta$  173.04, 172.16, 169.49, 148.55, 139.08, 136.43, 135.38, 129.27, 128.82, 128.51, 127.40, 123.90, 61.92, 60.92, 53.62, 51.05, 50.39, 35.87, 33.05, 32.28, 31.32, 27.66, 25.06, 21.91, 15.64; ESI MS:  $m/z$  1037.6 ( $\text{M} + \text{H}^+$ ); Anal. ( $\text{C}_{56}\text{H}_{72}\text{N}_{14}\text{O}_6 \cdot 2.2\text{CF}_3\text{COOH}$ ): C, H, N.

**(S,3S,3'S,6S,6'S,10aS,10a'S)-N,N'-((1S,1'S)-(1,1'-(1,4-phenylenebis(ethane-2,1-diyl))bis(1H-1,2,3-triazole-4,1-diyl))bis(phenylmethylene))bis(6-((S)-2-(methylamino)propanamido)-5-oxodecahydropyrrolo[1,2-a]azocine-3-carboxamide) (19)**—Yield 64% over two steps. Purity was determined by reverse phase analytical HPLC to be over 98%.  $^1\text{H}$  NMR ( $\text{D}_2\text{O}$ ):  $\delta$  7.28-7.15 (m, 6H), 7.12-7.02 (m, 6H), 6.50 (brs, 4H), 5.95 (s, 2H), 4.65 (m, 2H), 4.35 (m, 4H), 4.28 (m, 2H), 4.18 (m, 2H), 3.82 (m, 2H), 2.85 (m, 4H), 2.55 (s, 6H), 2.20-1.20 (m, 30H);  $^{13}\text{C}$  NMR ( $\text{D}_2\text{O}$ ):  $\delta$  172.64, 171.79, 169.10, 147.24, 138.78, 135.59, 128.76, 128.09, 127.00, 123.79, 61.55, 60.58, 56.78, 51.66, 50.66, 49.75, 35.57, 35.39, 32.65, 31.93, 30.90, 27.34, 24.68, 21.52, 15.23; ESI MS:  $m/z$  1065.6 ( $\text{M} + \text{H}^+$ ); Anal. ( $\text{C}_{58}\text{H}_{76}\text{N}_{14}\text{O}_6 \cdot 2.6\text{CF}_3\text{COOH}$ ): C, H, N.

**(S,3S,3'S,6S,6'S,10aS,10a'S)-N,N'-((1S,1'S)-(1,1'-(1,4-phenylenebis(propane-3,1-diyl))bis(1H-1,2,3-triazole-4,1-diyl))bis(phenylmethylene))bis(6-((S)-2-(methylamino)propanamido)-5-oxodecahydropyrrolo[1,2-a]azocine-3-carboxamide) (20)**—Yield 59% over two steps. Purity was determined by reverse phase analytical HPLC to be over 98%.  $^1\text{H}$  NMR ( $\text{D}_2\text{O}$ ):  $\delta$  7.52 (s, 2H), 7.22-7.05 (m, 10H), 6.55 (s, 4H), 6.02 (s, 2H), 4.65 (m, 2H), 4.32 (m,

2H), 4.15 (m, 2H), 4.01 (m, 4H), 3.85 (m, 2H), 2.58 (s, 6H), 2.25-1.20 (m, 38H);  $^{13}\text{C}$  NMR ( $\text{D}_2\text{O}$ ):  $\delta$  174.82, 172.49, 171.74, 147.88, 139.03, 138.15, 128.87, 128.25, 128.08, 127.04, 124.34, 61.53, 60.53, 56.81, 50.65, 49.99, 49.62, 35.57, 32.71, 31.94, 31.28, 30.93, 30.68, 27.34, 24.71, 21.55, 15.26; ESI MS:  $m/z$  1093.6 ( $\text{M} + \text{H}$ ) $^+$ ; Anal. ( $\text{C}_{60}\text{H}_{80}\text{N}_{14}\text{O}_6$  2.3 $\text{CF}_3\text{COOH}$ ): C, H, N.

**(S,3S,3'S,6S,6'S,10aS,10a'S)-N,N'-((1S,1'S)-(1,1'-(1,4-phenylenebis(hexane-6,1-diyl))bis(1H-1,2,3-triazole-4,1-diyl))bis(phenylmethylene))bis(6-((S)-2-(methylamino)propanamido)-5-oxodecahydropyrrolo[1,2-a]azocine-3-carboxamide) (21)**—Yield 64% over two steps. Purity was determined by reverse phase analytical HPLC to be over 98%.  $^1\text{H}$  NMR (300 MHz,  $\text{D}_2\text{O}$ ):  $\delta$  7.55 (s, 2H), 7.40-7.02 (m, 10H), 6.70 (s, 4H), 6.15 (s, 2H), 4.70 (m, 2H), 4.35 (m, 2H), 4.15 (m, 2H), 4.10-3.90 (m, 4H), 3.85 (m, 2H), 2.60 (s, 6H), 2.30-1.05 (m, 0.90-0.70 (m, 8H); ESI MS:  $m/z$  1177.7 ( $\text{M} + \text{H}$ ) $^+$ .

**(S,3S,3'S,6S,6'S,10aS,10a'S)-N,N'-((1S,1'S)-(1,1'-(1,4-phenylenebis(octane-8,1-diyl))bis(1H-1,2,3-triazole-4,1-diyl))bis(phenylmethylene))bis(6-((S)-2-(methylamino)propanamido)-5-oxodecahydropyrrolo[1,2-a]azocine-3-carboxamide) (22)**—Yield 66% over two steps. Purity was determined by reverse phase analytical HPLC to be over 98%.  $^1\text{H}$  NMR (300 MHz,  $\text{D}_2\text{O}$ ):  $\delta$  7.55 (s, 2H), 7.25-6.95 (m, 10H), 6.62 (s, 4H), 6.05 (s, 2H), 4.65 (m, 2H), 4.30 (m, 2H), 4.12 (m, 2H), 3.92 (m, 4H), 3.80 (m, 2H), 2.52 (s, 6H), 2.25-1.05 (m, 34H), 1.02-0.72 (m, 24H);  $^{13}\text{C}$  NMR ( $\text{D}_2\text{O}$ ):  $\delta$  171.91, 171.42, 168.93, 148.11, 139.59, 139.36, 128.66, 127.95, 127.04, 122.65, 61.32, 60.34, 56.79, 50.50, 49.81, 35.13, 32.83, 31.99, 31.33, 29.79, 19.16, 28.83, 27.20, 26.13, 24.88, 21.52, 15.28; ESI MS:  $m/z$  1233.8 ( $\text{M} + \text{H}$ ) $^+$ ; Anal. ( $\text{C}_{70}\text{H}_{100}\text{N}_{14}\text{O}_6$  2.9 $\text{CF}_3\text{COOH}$ ): C, H, N.

**(S,3S,3'S,6S,6'S,10aS,10a'S)-N,N'-((1S,1'S)-(1,1'-(decane-1,10-diyl))bis(1H-1,2,3-triazole-4,1-diyl))bis(phenylmethylene))bis(6-((S)-2-(methylamino)propanamido)-5-oxodecahydropyrrolo[1,2-a]azocine-3-carboxamide) (23)**—Yield 69% over two steps. Purity was determined by reverse phase analytical HPLC to be over 95%.  $^1\text{H}$  NMR (300 MHz,  $\text{D}_2\text{O}$ ):  $\delta$  7.67 (s, 2H), 7.26-7.10 (m, 10H), 6.07 (s, 2H), 4.73 (m, 2H), 4.28 (m, 2H), 4.25-4.10 (m, 6H), 3.83 (m, 2H), 2.54 (s, 6H), 2.20-1.92 (m, 4H), 1.86-1.30 (m, 30H), 0.98-0.80 (m, 12H);  $^{13}\text{C}$  NMR (75 MHz,  $\text{D}_2\text{O}$ ):  $\delta$  177.43, 173.05, 172.22, 148.26, 139.29, 129.28, 128.50, 127.43, 123.81, 62.00, 60.99, 57.20, 51.08, 50.76, 50.40, 36.00, 33.06, 32.36, 31.32, 29.52, 28.62, 28.26, 27.77, 25.76, 25.10, 21.93, 15.65; ESI MS:  $m/z$  1073.7 ( $\text{M} + \text{H}$ ) $^+$ .

**(S,3S,3'S,6S,6'S,10aS,10a'S)-N,N'-((1S,1'S)-(1,1'-(dodecane-1,12-diyl))bis(1H-1,2,3-triazole-4,1-diyl))bis(phenylmethylene))bis(6-((S)-2-(methylamino)propanamido)-5-oxodecahydropyrrolo[1,2-a]azocine-3-carboxamide) (24)**—Yield 65% over two steps. Purity was determined by reverse phase analytical HPLC to be over 95%.  $^1\text{H}$  NMR (300 MHz,  $\text{D}_2\text{O}$ ):  $\delta$  7.60 (s, 2H), 7.30-7.10 (m, 10H), 6.20 (s, 2H), 4.80 (m, 2H), 4.65 (m, 2H), 4.55-4.20 (m, 6H), 3.75 (m, 2H), 2.45 (s, 6H), 2.25-1.45 (m, 28H), 1.38 (d,  $J = 7.2$  Hz, 6H), 1.10-0.80 (m, 16H); ESI MS:  $m/z$  1101.7 ( $\text{M} + \text{H}$ ) $^+$ .

**(3S,6S,10aS)-6-((S)-2-(methylamino)propanamido)-N-((1-(4-(4-(4-(4-((S)-((3S,6S,10aS)-6-((S)-2-(methylamino)propanamido)-5-oxodecahydropyrrolo[1,2-a]azocine-3-carboxamido)(phenyl)methyl)-1H-1,2,3-triazol-1-yl)butyl)-1H-1,2,3-triazol-1-yl)butyl)-1H-1,2,3-triazol-4-yl)(phenyl)methyl)-5-oxodecahydropyrrolo[1,2-a]azocine-3-carboxamide (25)**—Yield 51% over two

steps. Purity was determined by reverse phase analytical HPLC to be over 95%. <sup>1</sup>H NMR (300 MHz, D<sub>2</sub>O): δ 7.87 (s, 1H), 7.71 (s, 2H), 7.30-7.11 (m, 10H), 6.05 (s, 2H), 4.64 (m, 2H), 4.35-4.16 (m, 10H), 3.81 (m, 2H), 2.60 (t, J = 6.2 Hz, 2H), 2.54 (s, 6H), 2.10 (m, 2H), 1.98 (m, 2H), 1.75-1.42 (m, 34H); <sup>13</sup>C NMR (75 MHz, D<sub>2</sub>O): δ 175.85, 174.79, 172.08, 150.63, 147.37, 141.60, 131.85, 131.09, 129.93, 128.50, 126.79, 64.57, 63.53, 59.73, 54.54, 53.66, 52.90, 52.59, 38.49, 35.57, 34.90, 33.93, 31.29, 30.32, 28.96, 28.65, 27.63, 27.38, 25.24, 24.49, 18.22; ESI MS: *m/z* 1112.7 (M + H)<sup>+</sup>.

**(S,3S,3'S,6S,6'S,10aS,10a'S)-N,N'-((1S,1'S)-(1,1'-((carbonylbis(azanediyl))bis(butane-4,1-diyl))bis(1H-1,2,3-triazole-4,1-diyl))bis(phenylmethylene))bis(6-((S)-2-(methylamino)propanamido)-5-oxodecahydropyrrolo[1,2-a]azocine-3-carboxamide) (26)**—Yield 42% over two steps. Purity was determined by reverse phase analytical HPLC to be over 95%. <sup>1</sup>H NMR (300 MHz, D<sub>2</sub>O): δ 7.75 (s, 2H), 7.40-7.20 (m, 10H), 6.16 (s, 2H), 4.74 (m, 2H), 4.36 (m, 2H), 4.32-4.20 (m, 6H), 3.89 (m, 2H), 2.95 (t, J = 6.6 Hz, 4H), 2.64 (s, 6H), 2.32-1.20 (m, 38H); ESI MS: *m/z* 1103.7 (M + H)<sup>+</sup>.

**(S,3S,3'S,6S,6'S,10aS,10a'S)-N,N'-((1S,1'S)-(1,1'-(oxybis(pentane-5,1-diyl))bis(1H-1,2,3-triazole-4,1-diyl))bis(phenylmethylene))bis(6-((S)-2-(methylamino)propanamido)-5-oxodecahydropyrrolo[1,2-a]azocine-3-carboxamide) (27)**—Yield 68% over two steps. Purity was determined by reverse phase analytical HPLC to be over 95%. <sup>1</sup>H NMR (300 MHz, D<sub>2</sub>O): δ 7.73 (s, 2H), 7.20-7.02 (m, 10H), 6.05 (s, 2H), 4.65 (m, 2H), 4.30 (m, 2H), 4.22-4.08 (m, 6H), 3.84 (m, 2H), 3.08 (m, 4H), 2.52 (s, 6H), 2.25-0.90 (m, 42H); <sup>13</sup>C NMR (75 MHz, D<sub>2</sub>O): δ 173.02, 172.13, 169.49, 147.91, 139.07, 129.31, 128.55, 127.41, 124.14, 70.25, 66.87, 61.93, 60.90, 57.18, 50.97, 50.22, 36.01, 33.08, 32.37, 31.40, 29.33, 28.23, 27.74, 25.11, 22.62, 21.97, 15.70; ESI MS: *m/z* 1089.7 (M + H)<sup>+</sup>.

**(S,3S,3'S,6S,6'S,10aS,10a'S)-N,N'-((1S,1'S)-(1,1'-((butane-1,4-diylbis(oxy))bis(ethane-2,1-diyl))bis(1H-1,2,3-triazole-4,1-diyl))bis(phenylmethylene))bis(6-((S)-2-(methylamino)propanamido)-5-oxodecahydropyrrolo[1,2-a]azocine-3-carboxamide) (28)**—Yield 63% over two steps. Purity was determined by reverse phase analytical HPLC to be over 95%. <sup>1</sup>H NMR (300 MHz, D<sub>2</sub>O): δ 7.77 (s, 2H), 7.22-7.08 (m, 10H), 6.05 (s, 2H), 4.65 (m, 2H), 4.37-4.22 (m, 6H), 4.16 (m, 2H), 3.82 (m, 2H), 3.48 (m, 4H), 3.08 (m, 4H), 2.52 (s, 6H), 2.16-1.42 (m, 30H), 1.01 (m, 4H); <sup>13</sup>C NMR (75 MHz, D<sub>2</sub>O): δ 173.11, 172.16, 169.49, 148.01, 139.10, 129.32, 128.56, 127.38, 124.62, 70.59, 68.39, 66.87, 61.96, 60.95, 57.19, 50.73, 50.24, 35.98, 33.09, 32.36, 31.40, 27.77, 25.43, 25.12, 21.96, 15.69; ESI MS: *m/z* 1077.6 (M + H)<sup>+</sup>.

**(3S,6S,10aS)-6-((S)-2-(methylamino)propanamido)-N-((1-(2-(2-(2-(4-((S)-((3S,6S,10aS)-6-((S)-2-(methylamino)propanamido)-5-oxodecahydropyrrolo[1,2-a]azocine-3-carboxamido)(phenyl)methyl)-1H-1,2,3-triazol-1-yl)ethoxy)ethoxy)ethyl)-1H-1,2,3-triazol-4-yl)(phenyl)methyl)-5-oxodecahydropyrrolo[1,2-a]azocine-3-carboxamide (29)**—Yield 67% over two steps. Purity was determined by reverse phase analytical HPLC to be over 95%. <sup>1</sup>H NMR (300 MHz, D<sub>2</sub>O): δ 7.58 (s, 2H), 7.29-7.13 (m, 10H), 6.08 (s, 2H), 4.70 (m, 2H), 4.38 (m, 4H), 4.27 (m, 2H), 4.22 (m, 2H), 3.85 (m, 2H), 3.73 (m, 4H), 3.32 (m, 4H), 3.25 (m, 4H), 2.58 (s, 6H), 2.25-1.48 (m, 22H), 1.40 (d, J = 7.0 Hz, 6H), 1.39 (m, 2H); <sup>13</sup>C NMR (75 MHz, D<sub>2</sub>O): δ 173.36, 172.32, 169.56, 148.12, 139.21, 129.32, 128.54, 127.40, 124.51, 69.98, 69.75, 68.97, 62.07, 61.07, 57.20, 51.13, 50.46, 50.41, 35.94, 33.01, 32.35, 31.31, 27.81, 25.07, 21.92, 15.63; ESI MS: *m/z* 1093.7 (M + H)<sup>+</sup>.

**tert-butyl ((S)-1-(((3S,6S,10aS)-3-(((R)-1-(4-(4-(4-azidobutyl)phenyl)butyl)-1H-1,2,3-triazol-4-yl)(phenyl)methyl)carbamoyl)-5-oxodecahydropyrrolo[1,2-a]azocin-6-yl)amino)-1-oxopropan-2-yl)(methyl)carbamate (32)**—CuSO<sub>4</sub> (10 mg, 0.04 mmol) and (+)-sodium l-ascorbate (20 mg, 0.1 mmol) in water (3 mL) was added to a solution of compound **31** (32 mg, 0.061 mmol) and 1,4-bis-(4-azidobutyl)benzene (60 mg, 0.22 mmol) in *tert*-butyl alcohol (5 mL). The mixture was stirred at room temperature overnight and then extracted with CH<sub>2</sub>Cl<sub>2</sub> (3 × 10 mL). After the combined organic layer was washed with brine, dried over Na<sub>2</sub>SO<sub>4</sub>, and evaporated, the residue was purified by chromatography to give **32** (30 mg, yield 62%). <sup>1</sup>H NMR (CDCl<sub>3</sub>): δ 8.01 (brd, J = 8.3 Hz, 1H), 7.40-7.20 (m, 6H), 7.15-7.02 (m, 4H), 6.90 (m, 1H), 6.29 (d, J = 8.3 Hz, 1H), 4.84 (m, 1H), 4.68 (m, 1H), 4.52 (brm, 1H), 4.31 (t, J = 7.1 Hz, 2H), 4.14 (m, 1H), 3.29 (t, J = 6.5 Hz, 2H), 2.81 (s, 3H), 2.62 (t, J = 7.2 Hz, 4H), 2.55 (m, 1H), 2.20-1.20 (m, 2H); <sup>13</sup>C NMR (CDCl<sub>3</sub>): δ 171.41, 170.53, 169.68, 148.06, 140.58, 139.50, 138.89, 128.60, 128.44, 128.38, 127.68, 127.39, 121.51, 59.94, 59.22, 51.33, 50.22, 50.01, 36.37, 35.97, 34.92, 34.69, 32.01, 30.13, 29.74, 28.48, 28.44, 28.41, 28.21, 24.93, 24.50, 23.13, 13.83; ESI MS: 797.5 (M + H)<sup>+</sup>.

**(3S,6S,10aS)-6-((R)-2-acetamido-3-(1H-indol-3-yl)propanamido)-N-((S)-1-(4-(4-(4-((S)-((3S,6S,10aS)-6-((R)-2-(methylamino)propanamido)-5-oxodecahydropyrrolo[1,2-a]azocin-3-carboxamido)(phenyl)methyl)-1H-1,2,3-triazol-1-yl)butyl)phenyl)butyl)-1H-1,2,3-triazol-4-yl)(phenyl)methyl)-5-oxodecahydropyrrolo[1,2-a]azocin-3-carboxamide (30)**—CuSO<sub>4</sub> (10 mg, 0.04 mmol) and (+)-sodium l-ascorbate (20 mg, 0.1 mmol) in H<sub>2</sub>O (5 mL) was added to a solution of compound **33** (15 mg, 0.026 mmol) and **32** (21 mg, 0.026 mmol) in *tert*-butyl alcohol (10 mL). The mixture was stirred at room temperature overnight and then extracted with CH<sub>2</sub>Cl<sub>2</sub> (3 × 30 mL). The combined organic layer was washed with brine, dried over Na<sub>2</sub>SO<sub>4</sub>, and evaporated. The residue was purified by chromatography to give a bis-triazole. To a solution of this bis-triazole in MeOH (5 mL) was added HCl (4N in 1,4-dioxane, 1 mL). The solution was stirred at room temperature overnight and then concentrated to furnish a crude product which was purified by C18 reversed phase semipreparative HPLC to give compound **30** (21.4 mg, yield 65%). <sup>1</sup>H NMR (D<sub>2</sub>O-CD<sub>3</sub>OD 1:1): δ 8.90 (m, 1H), 7.72 (s, 2H), 7.60 (m, 1H), 7.50-7.30 (m, 11H), 7.25-6.95 (m, 7H), 6.30-6.25 (m, 2H), 4.70 (m, 1H), 4.65 (m, 1H), 4.52 (m, 2H), 4.50-4.45 (m, 4H), 4.45-4.30 (m, 3H), 3.85 (m, 1H), 3.30 (m, 1H), 3.20 (m, 1H), 2.70 (m, 3H), 2.65 (m, 4H), 2.30-1.40 (m, 38H); ESI MS: *m/z* 1264.7 (M + H)<sup>+</sup>; Anal. (C<sub>71</sub>H<sub>89</sub>N<sub>15</sub>O<sub>7</sub> 1.7CF<sub>3</sub>COOH): C, H, N.

## II. Fluorescence polarization based assays for XIAP, cIAP-1 and cIAP-2 proteins

A set of sensitive and quantitative fluorescence polarization (FP)-based assays were used to determine the binding affinities of the designed Smac mimetics to XIAP BIR3, XIAP linker-BIR2-BIR3, cIAP-1 BIR3, cIAP-1 BIR2-BIR3 and cIAP-2 BIR3 proteins.

**Protein expression and purification**—Human XIAP BIR3 (residues 241–356) and linker-BIR2-BIR3 (residues 120–356) were cloned into a pET28 vector (Novagen) containing an N-terminal 6xHis tag. Protein was produced in *E. coli* BL21(DE3) cells grown at 37°C in 2xYT containing kanamycin to an OD<sub>600</sub> of 0.6.

Protein expression was induced by IPTG (0.4 mM) at 27°C for 4 hours. Cells were lysed by sonication in buffer containing Tris pH 7.5 (50 mM), NaCl (200 mM), ZnAc (50 μM), 0.1% βME and Leupeptin/Aprotin protease inhibitors. Protein was purified from the soluble fraction using Ni-NTA resin (QIAGEN) followed by gel filtration on a Superdex 75 column in Tris pH 7.5 (20 mM), NaCl (200 mM), ZnAc (50 μM), and dithiothreitol (DTT, 1 mM). After purification, DTT was added to a final concentration of 10 mM. Human cIAP-1 BIR3

(residues 253–363), cIAP-1 BIR2-BIR3 (residues 139–363) and cIAP2 BIR3 (residues 238–349) were cloned into pHis-TEV vector, produced and purified using the same method as for the XIAP protein.

**FP-based binding assays**—A fluorescently labeled Smac mimetic (Smac-2F) was used in FP assays to determine the binding affinities of our Smac mimetics to XIAP BIR3, cIAP-1 BIR3, cIAP-2 BIR3, and cIAP-1 BIR2-BIR3 proteins.<sup>33</sup> The  $K_d$  values of Smac-2F to XIAP BIR3, cIAP-1 BIR3, cIAP-2 BIR3, and cIAP-1 BIR2-BIR3 were determined by monitoring the total fluorescence polarization of mixtures composed with fluorescent tracer at a fixed concentration and proteins with increasing concentrations up to full saturation. Fluorescence polarization values were measured using the Infinite M-1000 plate reader (Tecan U.S., Research Triangle Park, NC) in Microfluor 2 96-well, black, round-bottom plates (Thermo Scientific). To each well, SMAC-2F (2nM, 1nM, 1nM, and 1nM for experiments with XIAP BIR3, cIAP-1BIR3, cIAP-2 BIR3, and cIAP-1 BIR2-BIR3, respectively) and increasing concentrations of protein were added to a final volume of 125  $\mu$ l in the assay buffer (100mM potassium phosphate, pH 7.5, 100  $\mu$ g/ml bovine  $\gamma$ -globulin, 0.02% sodium azide, Invitrogen, with 4% DMSO). Plates were incubated at room temperature for 2–3 hours and mixed with gentle shaking to assure equilibrium. The polarization values in millipolarization units (mP) were measured at an excitation wavelength of 485 nm and an emission wavelength of 530 nm. Equilibrium dissociation constants ( $K_d$ ) were then calculated by fitting the sigmoidal dose-dependent FP increases as a function of protein concentrations using Graphpad Prism 5.0 software (Graphpad Software, San Diego, CA).

The  $K_i$  values of inhibitors were determined through an inhibitor dose-dependent competitive binding experiment in which serial dilutions of inhibitor competed against fixed concentration of the fluorescent tracer for binding to a fixed concentration of the protein (typically 2 to 3 times the  $K_d$  values determined above). Mixtures of 5  $\mu$ l of the tested compounds in DMSO and 120  $\mu$ l of preincubated protein/tracer complex in the assay buffer (100mM potassium phosphate, pH 7.5, 100  $\mu$ g/ml bovine  $\gamma$ -globulin, 0.02% sodium azide, Invitrogen) were added into assay plates and incubated at room temperature for 3 h with gentle shaking. Final concentrations of proteins and tracers were 10nM and 2nM, 3nM and 1nM, 5nM and 1nM, and 6nM and 1nM for assays for XIAP BIR3, cIAP-1 BIR3, cIAP-2 BIR3, and cIAP-1 BIR2-BIR3, respectively. Negative controls containing protein/tracer complex only (equivalent to 0% inhibition), and positive controls containing only free tracers (equivalent to 100% inhibition), were included in each assay plate. FP values were measured as described above.  $IC_{50}$  values were determined by nonlinear regression fitting of the competition curves. The  $K_i$  values of competitive inhibitors were calculated using the derived equation described previously<sup>41</sup>, based upon the measured  $IC_{50}$  values, the  $K_d$  values of the tracer to different proteins, and the concentrations of the proteins and tracers in the competitive assays.

The FP-based assay for XIAP linker-BIR2-BIR3 protein has been described in detail.<sup>42</sup> In this assay, a bivalent fluorescently tagged peptidic Smac mimetic (Smac-1F) was used as the fluorescent tracer in this FP-based binding assay.<sup>42</sup>

### III. Caspase-9 and Caspase-3 activity assays

For the caspase-9 activity assay, the enzymatic activity of active recombinant caspase-9 (Enzo Life Sciences) was evaluated by the caspase-Glo 9 Assay kit from Promega. 2.5  $\mu$ L of a solution of the compound in caspase assay buffer (CAB, 50 mM of HEPES, 100 mM of NaCl, 1 mM of EDTA with 0.1% of CHAPS and 10% of Glycerol, pH 7.4) containing 20% DMSO was mixed with 7.5  $\mu$ L of XIAP protein containing linker-BIR2-BIR3 and pre-

incubated for 15 minutes, followed by addition of 2.5  $\mu\text{L}$  of active caspase-9 solution in CAB. This mixture was incubated at room temperature for 15 minutes. Luminogenic Z-LEHD substrate was added with 1:1 ratio to give final concentrations of XIAP and Caspase-9 of 500 nM and 2.5 unit/reaction (according to the manufacturer's instructions), respectively. This mixture was incubated at room temperature without light for 1 h, and luminescence from the substrate cleavage was then determined by Tecan Infinite M-1000 multimode plate reader.

For caspase-3 activity assay, the enzymatic activity of Caspase-3 was determined using the Caspase-3 Fluorescent Assay kit (BD Biosciences). 5  $\mu\text{L}$  of a solution of the compound in CAB with 20% DMSO was pre-incubated with 15  $\mu\text{L}$  of XIAP linker-BIR2-BIR3 protein for 15 minutes followed by addition of 5  $\mu\text{L}$  of active Caspase-3 solution and the mixture was incubated at room temperature for 15 minutes. Fluorescent Ac-DEVD-AFC substrate was added at 1:1 ratio to give final concentrations of XIAP, Caspase-3, and Ac-DEVD-AFC at 20 nM, 40ng/mL, and 125ng/mL, respectively. Fluorescence from the cleavage of substrate was measured by Tecan Infinite M-1000 multimode plate reader using an excitation wavelength of 400 nm and an emission wavelength of 505 nm. The reaction was monitored for 1–2 h.

#### IV. Cell growth inhibition assay

The MDA-MB-231 cell line was purchased from the American Type Culture Collection. Cells were seeded in 96-well flat bottom cell culture plates at a density of  $3\text{--}4 \times 10^3$  cells/well and grown overnight, then incubated with a compound at different concentrations. The rate of cell growth inhibition after treatment with different concentrations of a compound was determined by assaying with (2-(2-methoxy-4-nitrophenyl)-3-(4-nitrophenyl)-5-(2,4-disulfophenyl)-2H-tetrazolium monosodium salt (WST-8; Dojindo Molecular Technologies Inc., Gaithersburg, Maryland). WST-8 was added to each well to a final concentration of 10%, and then the plates were incubated at 37°C for 2–3 h. The absorbance of the samples was measured at 450 nm using a TECAN ULTRA Reader. The concentrations of the compounds that inhibited cell growth by 50% ( $\text{IC}_{50}$ ) was calculated by comparing absorbance in the untreated cells and the treated cells.

#### V. Western blot analysis

Cells were harvested and washed with cold PBS. Cell pellets were lysed in double lysis buffer (DLB; 50 mmol/L Tris, 150 mmol/L sodium chloride, 1 mmol/L EDTA, 0.1% SDS and 1% NP-40) in the presence of PMSF (1 mmol/L) and protease inhibitor cocktail (Roche) for 10 min on ice, then centrifuged at 13,000 rpm at 4°C for 10 min. Protein concentrations were determined using a Bio-Rad protein assay kit (Bio-Rad Laboratories). Proteins were electrophoresed onto a 4% – 20% gradient SDS-PAGE (Invitrogen) and then transferred to PVDF membranes. After blocking in 5% milk, the membranes were incubated with a specific primary antibody, washed, and incubated with horseradish peroxidase-linked secondary antibody (Amersham). The signals were visualized with a Chemiluminescent HRP antibody detection reagent (Denville Scientific). When indicated, the blots were stripped and reprobed with a different antibody. Primary antibody against cleaved caspase 3 was purchased from Stressgen Biotechnologies; Primary antibodies against cIAP-1 and cIAP-2 were purchased from R&D systems; Primary antibody against XIAP was purchased from BD Biosciences; Primary antibodies against PARP and  $\beta$ -actin were purchased from Cell Signaling Technology.

#### VI. Determination of intracellular concentrations of Smac mimetics

MDA-MB-231 cells were cultured in 100 mm cell culture dishes at a density of  $10\text{--}15 \times 10^6$  cells/dish and incubated with 300 nM of a compound at 37°C for 5s, 30s, 60s, 1 h, 3 h, or 6

h. After incubation, culture medium with a compound was aspirated and the adherently growing cells were washed with cold PBS (10mL × 3, 10 seconds/wash). Cells were then scraped directly into 2 mL of pure methanol. After methanol was removed by evaporation, cell pellets were reconstituted in 100 µL of deionized water. To complete the cell lyses, cell suspensions were sonicated in a water bath for 10 minutes followed by centrifuge at 14,000 RPM for 5 minutes. Supernatant aliquot (20 µL) was mixed with 60 µL of acetonitrile (containing internal standard at 300nM) to precipitate proteins. Supernatant (5 µL) was injected for LC-MS/MS analysis after centrifuging at 14,000 RPM for 5 min. Total protein concentrations of the supernatant were determined by Micro BCA protein assay kit from Pierce. Compound concentrations determined by LC-MS/MS were normalized to the total protein concentrations to compensate the cell number difference of each cell dish.

Quantitative LC-MS/MS analysis was conducted using an Agilent 1200 HPLC system coupled to an API 3200 mass spectrometer (Applied Biosystems, MDS Sciex Toronto, Canada) equipped with an API electrospray ionization (ESI) source.

Aliquots (5 µL) were injected onto a reversed-phase column [5 cm × 2.1 mm I.D., packed with 3.5 µm Zorbax Bonus-RP (Agilent)]. The mobile phase consisted of 0.1% formic acid in water (A) and 0.1% formic acid in acetonitrile (B). The mobile phase A was held at 10% for 0.5 min, increased from 10% to 98% over 0.1 min, held at 98% for an additional 4 min, and then immediately stepped back down to 10% for re-equilibration. The mobile phase was eluted at 0.4 mL/min.

## VII. *In vivo* antitumor efficacy study

Female severe combined immunodeficiency (SCID) mice were injected subcutaneously with  $5 \times 10^6$  MDA-MB-231 cells in 50% Matrigel per mouse. Treatment started when the tumors reached an average volume of 150 mm<sup>3</sup> on day 26. Mice were treated with vehicle (9 mice per group), taxotere at 7.5mg/kg intravenously on treatment days 2 & 9 (8 per group), compound **27** at 1 or 5mg/kg given intravenously on days 1–5 & 8–12 with 8 mice per group. Tumor sizes and animal weights were measured 3 times a week during the treatment and twice a week after the treatment. Data are presented as mean tumor volumes ± SEM. Statistical analyses were performed by two-way ANOVA and unpaired two-tailed t test, using Prism (version 4.0, GraphPad, La Jolla, CA).  $P < 0.05$  was considered statistically significant. The efficacy experiment was performed under the guidelines of the University of Michigan Committee for Use and Care of Animals.

## Acknowledgments

We are grateful for the financial support from the Breast Cancer Research Foundation, the National Cancer Institute, NIH (R01CA109025 and R01CA127551), the Susan G. Koman Foundation, Ascenta Therapeutics, and University of Michigan Cancer Center Core grant from the National Cancer Institute, NIH (P30CA046592). The authors thank Dr. G.W.A. Milne for his critical reading of the manuscript and many useful suggestions and Ms. Karen Kreutzer for her excellent secretary assistance.

## Abbreviations

<b>IAP</b>	Inhibitor of apoptotic protein
<b>XIAP</b>	X-linked IAP
<b>cIAP</b>	cellular IAP
<b>Smac</b>	second mitochondria derived activator of caspases
<b>BIR</b>	baculoviral IAP repeat

<b>PARP</b>	poly(ADPribose) polymerase
<b>FP</b>	fluorescence polarization
<b>mP</b>	millipolarization units
<b>TRAF1</b>	tumor necrosis factor associated factor 2

## References

- Hanahan D, Weinberg RA. The hallmarks of cancer. *Cell*. 2000; 100:57–70. [PubMed: 10647931]
- Lowe SW, Lin AW. Apoptosis in cancer. *Carcinogenesis*. 2000; 21:485–495. [PubMed: 10688869]
- Nicholson DW. From bench to clinic with apoptosis-based therapeutic agents. *Nature*. 2000; 407:810–816. [PubMed: 11048733]
- Salvesen GS, Duckett CS. Apoptosis: IAP proteins: blocking the road to death's door. *Nat Rev Mol Cell Biol*. 2002; 3:401–410. [PubMed: 12042762]
- Deveraux QL, Reed JC. IAP family proteins—suppressors of apoptosis. *Genes Dev*. 1999; 13:239–252. [PubMed: 9990849]
- Holcik M, Gibson H, Korneluk RG. XIAP: Apoptotic brake and promising therapeutic target. *Apoptosis*. 2001; 6:253–261. [PubMed: 11445667]
- Shiozaki EN, Shi Y. Caspases, IAPs and Smac/DIABLO: mechanisms from structural biology. *Trends Biochem Sci*. 2004; 29:486–494. [PubMed: 15337122]
- Srinivasula SM, Ashwell JD. IAPs: what's in a name? *Mol Cell*. 2008; 30:123–135. [PubMed: 18439892]
- Gyrd-Hansen M, Meier P. IAPs: from caspase inhibitors to modulators of NF-kappaB, inflammation and cancer. *Nat Rev Cancer*. 2010; 10:561–574. [PubMed: 20651737]
- Mehrotra S, Languino LR, Raskett CM, Mercurio AM, Dohi T, Altieri D. C IAP Regulation of Metastasis. *Cancer Cell*. 2010; 17:53–64. [PubMed: 20129247]
- LaCasse EC, Mahoney DJ, Cheung HH, Plenchette S, Baird S, Korneluk RG. IAP-targeted therapies for cancer. *Oncogene*. 2008; 27:6252–6275. [PubMed: 18931692]
- Vucic D, Fairbrother WJ. The inhibitor of apoptosis proteins as therapeutic targets in cancer. *Clin Cancer Res*. 2007; 13:5995–6000. [PubMed: 17947460]
- Fulda S. Inhibitor of apoptosis proteins as targets for anticancer therapy. *Expert Rev Anticancer Ther*. 2007; 7:1255–1264. [PubMed: 17892425]
- Du C, Fang M, Li Y, Li L, Wang X. Smac, a mitochondrial protein that promotes cytochrome c-dependent caspase activation by eliminating IAP inhibition. *Cell*. 2000; 102:33–42. [PubMed: 10929711]
- Verhagen AM, Ekert PG, Pakusch M, Silke J, Connolly LM, Reid GE, Moritz RL, Simpson RJ, Vaux DL. Identification of DIABLO, a mammalian protein that promotes apoptosis by binding to and antagonizing IAP proteins. *Cell*. 2000; 102:43–53. [PubMed: 10929712]
- Wu G, Chai J, Suber TL, Wu JW, Du C, Wang X, Shi Y. Structural basis of IAP recognition by Smac/DIABLO. *Nature*. 2000; 408:1008–1012. [PubMed: 11140638]
- Liu Z, Sun C, Olejniczak ET, Meadows R, Betz SF, Oost T, Herrmann J, Wu JC, Fesik SW. Structural basis for binding of Smac/DIABLO to the XIAP BIR3 domain. *Nature*. 2000; 408:1004–1008. [PubMed: 11140637]
- Huang Y, Rich RL, Myszka DG, Wu H. Requirement of both the second and third BIR domains for the relief of X-linked inhibitor of apoptosis protein (XIAP)-mediated caspase inhibition by Smac. *J Biol Chem*. 2003; 278:49517–49522. [PubMed: 14512414]
- Samuel T, Welsh K, Lober T, Togo SH, Zapata JM, Reed JC. Distinct BIR domains of cIAP1 mediate binding to and ubiquitination of tumor necrosis factor receptor-associated factor 2 and second mitochondrial activator of caspases. *J Biol Chem*. 2006; 281:1080–1090. [PubMed: 16282325]
- Wang S. Design of Small-Molecule Smac Mimetics as IAP Antagonists. *Curr Top Microbiol Immunol*. 2010 Nov 12. [Epub ahead of print].

21. Sun H, Nikolovska-Coleska Z, Yang CY, Qian D, Lu J, Qiu S, Bai L, Peng Y, Cai Q, Wang S. Design of small-molecule peptidic nonpeptidic Smac mimetics. *Acc Chem Res.* 2008; 41:1264–1277. [PubMed: 18937395]
22. Mannhold R, Fulda S, Carosati E. IAP antagonists: promising candidates for cancer therapy. *Drug Discovery Today.* 2010; 15:210–219. [PubMed: 20096368]
23. Cai Q, Haiying Sun H, Peng Y, Lu J, Nikolovska-Coleska Z, McEachern D, Liu L, Qiu S, Yang C-Y, Miller R, Yi H, Zhang T, Sun D, Kang S, Guo M, Leopold L, Yang D, Wang S. A potent and orally active antagonist (SM-406/AT-406) of multiple inhibitor of apoptosis proteins (IAPs) in clinical development for cancer treatment. *J Med Chem.* 2011 (in press).
24. Sun H, Nikolovska-Coleska Z, Yang CY, Xu L, Liu M, Tomita Y, Pan H, Yoshioka Y, Krajewski K, Roller PP, Wang S. Structure-Based Design of Potent, Conformationally Constrained Smac Mimetics. *J Am Chem Soc.* 2004; 126:16686–16687. [PubMed: 15612682]
25. Sun H, Nikolovska-Coleska Z, Yang CY, Xu L, Tomita Y, Krajewski K, Roller PP, Wang S. Structure-based design, synthesis, and evaluation of conformationally constrained mimetics of the second mitochondria-derived activator of caspase that target the X-linked inhibitor of apoptosis protein/caspase-9 interaction site. *J Med Chem.* 2004; 47:4147–4150. [PubMed: 15293984]
26. Li L, Thomas RM, Suzuki H, De Brabander JK, Wang X, Harran PG. A small molecule Smac mimic potentiates TRAIL- and TNF alpha-mediated cell death. *Science.* 2004; 305:1471–1474. [PubMed: 15353805]
27. Oost TK, Sun C, Armstrong RC, Al-Assaad AS, Betz SF, Deckwerth TL, Ding H, Elmore SW, Meadows RP, Olejniczak ET, Oleksijew A, Oltersdorf T, Rosenberg SH, Shoemaker AR, Tomaselli KJ, Zou H, Fesik SW. Discovery of potent antagonists of the antiapoptotic protein XIAP for the treatment of cancer. *J Med Chem.* 2004; 47:4417–4426. [PubMed: 15317454]
28. Sun H, Nikolovska-Coleska Z, Lu J, Qiu S, Yang CY, Gao W, Meagher J, Stuckey J, Wang S. Design, synthesis, and evaluation of a potent, cell-permeable, conformationally constrained second mitochondria derived activator of caspase (Smac) mimetic. *J Med Chem.* 2006; 49:7916–7920. [PubMed: 17181177]
29. Sun H, Stuckey JA, Nikolovska-Coleska Z, Qin D, Meagher JL, Qiu S, Lu J, Yang CY, Saito NG, Wang S. Structure-based design, synthesis, evaluation, and crystallographic studies of conformationally constrained Smac mimetics as inhibitors of the X-linked inhibitor of apoptosis protein (XIAP). *J Med Chem (Article).* 2008; 51(22):7169–7180.
30. Peng Y, Sun H, Nikolovska-Coleska Z, Qiu S, Yang CY, Lu J, Cai Q, Yi H, Wang S. Design, Synthesis and Evaluation of Potent and Orally Bioavailable Diazabicyclic Smac Mimetics. *J Med Chem.* 2008; 51:8158–8162. [PubMed: 19049347]
31. Zhang B, Nikolovska-Coleska Z, Zhang Y, Bai L, Qiu S, Yang CY, Sun H, Wang S, Yikang Wu Y. *J Med Chem.* 2008; 51:7352–7355. [PubMed: 19012392]
32. Sun W, Nikolovska-Coleska Z, Qin D, Sun H, Yang CY, Bai L, Qiu S, Ma D, Wang S. Design, Synthesis and Evaluation of Potent, Non-Peptidic Smac Mimetics. *J Med Chem.* 2009; 52:593–596. [PubMed: 19138149]
33. Sun H, Lu J, Liu L, Yi H, Qiu S, Yang CY, Deschamps JR, Wang S. Nonpeptidic and Potent Small-Molecule Inhibitors of cIAP-1/2 and XIAP Proteins. *J Med Chem.* 2010; 53:6361–6367. [PubMed: 20684551]
34. Zobel K, Wang L, Varfolomeev E, Franklin MC, Elliott LO, Wallweber HJ, Okawa DC, Flygare JA, Vucic D, Fairbrother WJ, Deshayes K. Design, synthesis, and biological activity of a potent Smac mimetic that sensitizes cancer cells to apoptosis by antagonizing IAPs. *ACS Chem Biol.* 2006; 1:525–533. [PubMed: 17168540]
35. Sun H, Nikolovska-Coleska Z, Lu J, Meagher JL, Yang CY, Qiu S, Tomita Y, Ueda Y, Jiang S, Krajewski K, Roller PP, Stuckey JA, Wang S. Design synthesis and characterization of a potent nonpeptide cell-permeable bivalent Smac mimetic that concurrently targets both the BIR2 BIR3 domains in XIAP. *J Am Chem Soc.* 2007; 129:15279–15294. [PubMed: 17999504]
36. Varfolomeev E, Blankenship JW, Wayson SM, Fedorova AV, Kayagaki N, Garg P, Zobel K, Dynek JN, Elliott LO, Wallweber HJ, Flygare JA, Fairbrother WJ, Deshayes K, Dixit VM, Vucic D. IAP antagonists induce autoubiquitination of c-IAPs, NF-kappaB activation, and TNFalpha-dependent apoptosis. *Cell.* 2007; 131:669–681. [PubMed: 18022362]

37. Vince JE, Wong WW, Khan N, Feltham R, Chau D, Ahmed AU, Benetatos CA, Chunduru SK, Condon SM, McKinlay M, Brink R, Leverkus M, Tergaonkar V, Schneider P, Callus BA, Koentgen F, Vaux DL, Silke J. IAP antagonists target cIAP1 to induce TNFalpha-dependent apoptosis. *Cell*. 2007; 131:682–693. [PubMed: 18022363]
38. Petersen SL, Wang L, Yalcin-Chin A, Li L, Peyton M, Minna J, Harran P, Wang X. Autocrine TNFalpha signaling renders human cancer cells susceptible to Smac-mimetic-induced apoptosis. *Cancer Cell*. 2007; 12:445–456. [PubMed: 17996648]
39. Lu J, Bai L, Sun H, Nikolovska-Coleska Z, McEachern D, Qiu S, Miller RS, Yi H, Shangary S, Sun Y, Meagher JL, Stuckey JA, Wang S. SM-164: A novel, bivalent Smac mimetic that induces apoptosis and tumor regression by concurrent removal of the blockade of cIAP-1/2 and XIAP. *Cancer Research*. 2008; 68:9384–9393. [PubMed: 19010913]
40. Nikolovska-Coleska Z, Meagher JL, Jiang S, Yang CY, Qiu S, Roller PP, Stuckey JA, Wang S. Interaction of a cyclic, bivalent smac mimetic with the x-linked inhibitor of apoptosis protein. *Biochemistry*. 2008; 47:9811–9824. [PubMed: 18717598]
41. Nikolovska-Coleska Z, Wang R, Fang X, Pan H, Tomita Y, Li P, Roller PP, Krajewski K, Saito NG, Stuckey JA, Wang S. Development and optimization of a binding assay for the XIAP BIR3 domain using fluorescence polarization. *Analytical Biochemistry*. 2004; 332:261–273. [PubMed: 15325294]
42. Nikolovska-Coleska Z, Meagher JL, Jiang S, Kawamoto SA, Gao W, Yi H, Qin D, Roller PP, Stuckey JA, Wang S. Design and characterization of bivalent Smac-based peptides as antagonist of XIAP and development and validation of a fluorescence polarization assay for XIAP containing both BIR2 and BIR3 domains. *Analytical Biochemistry*. 2008; 374:87–98. [PubMed: 18023397]

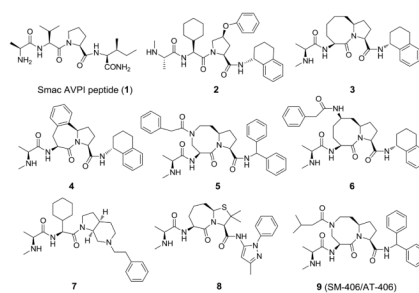


**Figure 1.**  
Chemical structures of Smac AVPI peptide and previously reported monovalent Smac mimetics.

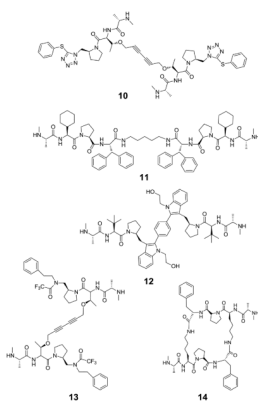
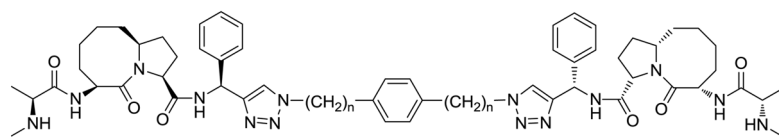


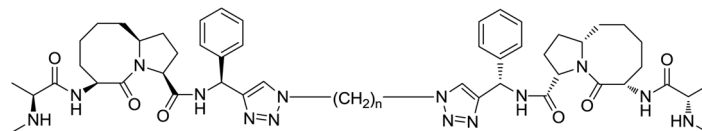
**Figure 2.**  
Chemical structures of previously reported bivalent Smac mimetics.



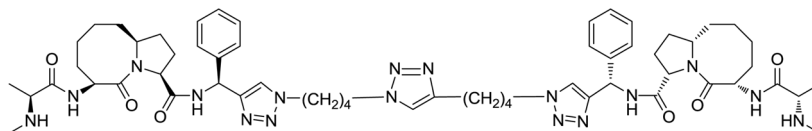
**Figure 3.**  
Chemical structures of previously reported monovalent Smac mimetic **15**, bivalent Smac mimetic **16** and an inactive analogue **17**.



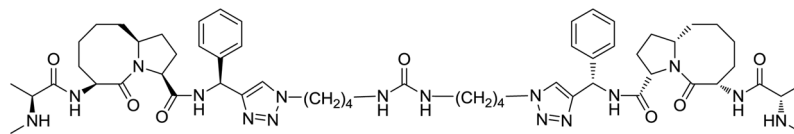
**18, n = 1; 19, n = 2; 20, n = 3; 21, n = 6; 22, n = 8**



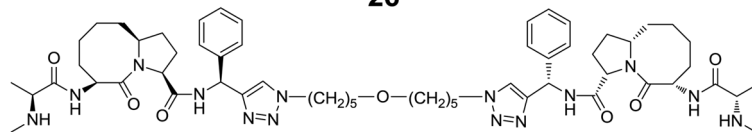
**23, n = 10; 24, n = 12**



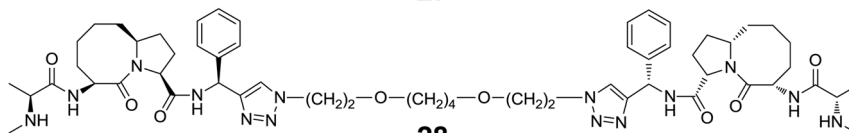
**25**



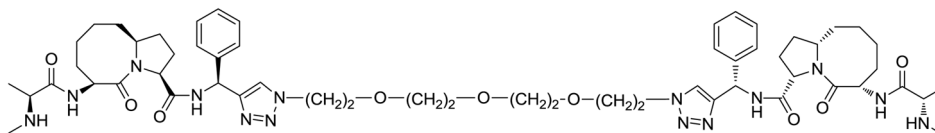
**26**



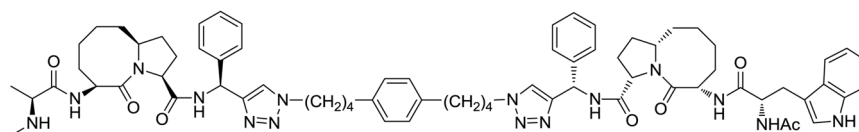
**27**



**28**

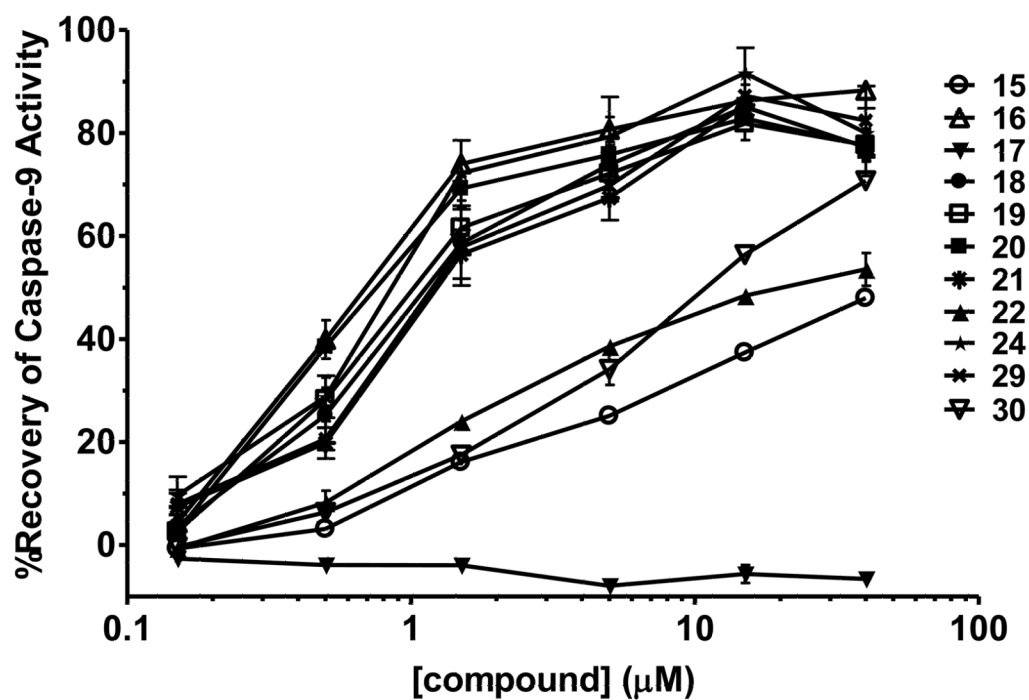


**29**

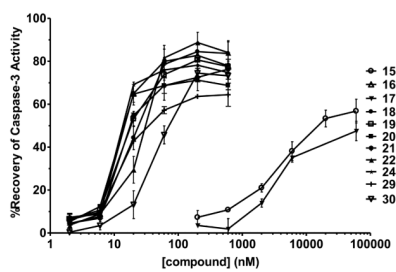


**30**

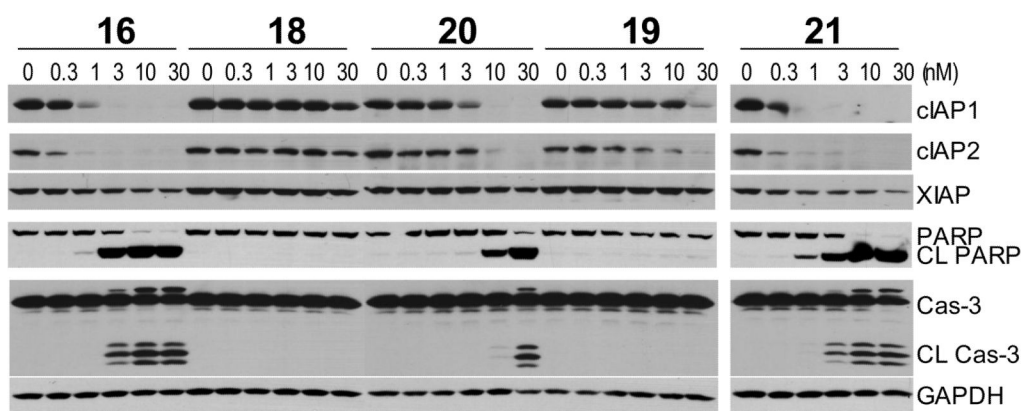
**Figure 4.**  
Chemical structures of new bivalent Smac mimetics.



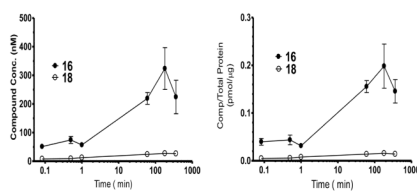
**Figure 5.** Functional antagonism of Smac mimetics against XIAP linker-BIR2-BIR3 in a cell-free caspase-9 functional assay. Data shown in the figure are averages and standard deviations of duplicate wells in assay plates, and the figure is the representative of three independent experiments.



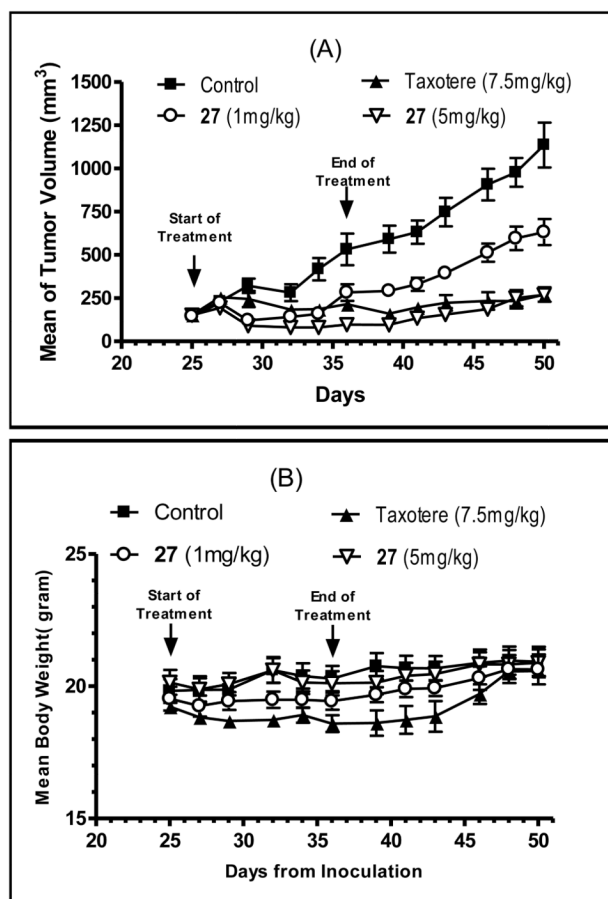
**Figure 6.** Functional antagonism of Smac mimetics against XIAP linker-BIR2-BIR3 in a cell-free caspase-3 functional assay. Data shown in the figure are averages and standard deviations of duplicate wells in assay plates and the figure is representative of three independent experiments.



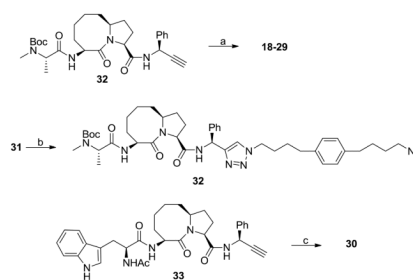
**Figure 7.** Induction of cIAP-1, cIAP-2 and XIAP degradation, cleavage of PARP, and processing of caspase-3 by compounds **16**, **18**, **19**, **20** and **21** in the MDA-MB-231 cell line. Cells were treated with different concentrations of Smac mimetics for 24 h and cIAP-1, cIAP-2, XIAP, cleaved PARP (CL PARP), and cleaved caspase-3 (CL C3) were probed by Western blot analysis.



**Figure 8.** (A) Concentrations of compounds **16** and **18** in 100  $\mu\text{L}$  of cell lysates; and (B) amount of compounds per  $\mu\text{g}$  of total proteins. 300nM of each compound was incubated with  $10\text{--}15 \times 10^6$  MDA-MB-231 cells for different times. After being washed by PBS, cells were lysed and resuspended in 100  $\mu\text{L}$  of deionized water. Compound concentrations and protein concentrations were determined by LC-MS/MS and Micro BCA protein assay, respectively. Data shown in the figure are averages and standard deviations of three independent experiments.



**Figure 9.** Antitumor activity of compound **27** in the MDA-MB-231 xenograft model in SCID mice. (A). Mean tumor volume. (B). Mean animal weight. Treatment started when the tumors reached an average volume of 150mm<sup>3</sup> on day 26. Treatment groups consisted of vehicle control (9 mice per group), Taxotere 7.5mg/kg given intravenously on treatment days 2 and 9 with 8 mice per group, compound **27** at 1 mg/kg or 5mg/kg given intravenously on days 1–5 and 8–12, with 8 mice per group.

**Scheme 1.**

Synthesis of bivalent Smac mimetics.

**Reagents and conditions:** (a) i. bis-azides,  $\text{CuSO}_4$ , (+)-sodium -L-ascorbate, *tert*-butanol- $\text{H}_2\text{O}$  2:1; ii. 4 N HCL in 1,4-dioxane, MeOH; (b) 1,4-bis-(4-azido-butyl)-benzene (5 eq),  $\text{CuSO}_4$ , (+)-sodium-L-ascorbate, *tert*-butanol- $\text{H}_2\text{O}$  2:1, 62%; (c) i. **33**,  $\text{CuSO}_4$ , (+)-sodium -L-ascorbate, *tert*-butanol- $\text{H}_2\text{O}$  2:1; ii 4 N HCL in 1,4-dioxane, MeOH

Table 1

Binding affinities of Smac mimetics to XIAP BIR3, XIAP Linker-BIR2-BIR3, cIAP-1 BIR3, cIAP1 BIR2-BIR3 and cIAP2 proteins, and inhibition of cell growth in the MDA-MB-231 cancer cell line. Standard deviation was calculated with 3 independent experiments.

Cmpd	Binding Affinities to IAP Proteins												Cell Growth Inhibition	
	XIAP BIR3		XIAP L-BIR2-BIR3		cIAP-1 BIR3		cIAP-1 BIR2-BIR3		cIAP-2 BIR3		MDA-MB-231			
	IC <sub>50</sub> (nM)	K <sub>i</sub> (nM)	IC <sub>50</sub> (nM)	K <sub>i</sub> (nM)	IC <sub>50</sub> (nM)	K <sub>i</sub> (nM)	IC <sub>50</sub> (nM)	K <sub>i</sub> (nM)	IC <sub>50</sub> (nM)	K <sub>i</sub> (nM)	IC <sub>50</sub> (nM)	K <sub>i</sub> (nM)		
15	819±126	248±36	1240±42	408±14	38±7	6.8±2	60±12	18±3	70±10	18±2.5	633±32			
16	153±5	45±2	7.5±0.8	2±0.2*	4.6±0.7	<1	5.7±3.2	1.5±0.8	8.5±4.2	2±1	3.3±0.4			
17	> 50,000	>10,000	> 50,000	> 10,000	> 50,000	> 9000	> 10,000	>3,000	> 50,000	>10,000	>100,000			
18	426±36	128±9	16±3	5±1*	10±3	2±0.6	8.8±6.0	2±1.5	24±7	6±2	152±13			
19	190±4	56±1	10±4	3±1*	6.2±2.5	1±0.5	5.7±1.6	1.5±0.4	8.6±3.9	2±1	150±28			
20	187±25	55±6	6.0±0.2	1.5±0.1*	2.6±0.1	<1	3.6±1.9	1±0.5	5.0±2.7	1.2±0.6	10.6±0.5			
21	177±33	52±10	7.9±2.9	2±1*	5.4±2.3	1±0.5	9.5±3.5	3±1	8.6±1.8	2±0.4	1.6±0.1			
22	613±20	185±5	17±4	4±1*	13±3	2.5±0.6	7.3±4.7	2±1	13±4	3±1	2.7±0.2			
23	134±11	39±3	6.4±2.7	2±1*	2.8±0.8	<1	9.0±3.2	3±1	8.2±1.9	2±0.4	5.7±0.5			
24	131±20	38±6	6.6±1.9	2±1*	3.2±0.8	<1	9.2±3.9	3±1	8.7±0.9	2±0.2	1.2±0.3			
25	161±18	47±6	5.3±2.5	1±0.5*	6.2±0.7	1±0.2	6.5±1.5	2±0.5	11±1	2.5±0.2	107±2			
26	216±14	64±5	5.4±1.8	1±0.3*	6.8±0.9	1±0.2	7.4±3.3	2±1	14±3	3±0.8	263±8			
27	212±21	63±6	5.4±2.0	1±0.4*	4.9±2.4	<1	7.4±2.6	2±0.7	11±2	2.5±0.4	19.6±5.5			
28	280±39	83±12	8.2±0.9	3±0.5*	7.5±1.6	1±0.5	9.8±3.2	3±1	17±4	4±1	175±53			
29	523±20	157±6	14±3	4±1*	13±3	2±0.5	14±4	3±1	27±6	7±2	225±17			
30	618±46	186±12	280±3	88±1	16±11	3±2	23±14	6±3	43±22	11±5	669±13			

\* Exceeding assay limit and K<sub>i</sub> value is an estimated.

Intracellular concentrations of bivalent Smac mimetics, 10–15×10<sup>6</sup> MDA-MB-231 cells were treated with a compound at 300 nM for 1 minute and 3 hours, respectively, and then lysed in 100 μL of water. Concentrations for each compound in resuspended cell lysates were determined by LC-MS/MS. Standard deviation was calculated with 3 independent experiments

**Table 2**

Compounds	16	18	19	20	29
Concentration of the compound in resuspended cell lysate (nM)	106±18	21.2±4.7	11.4±1.6	48.1±4.6	6.7
	541±130	75.2±3.1	67.7±10.1	196±10.1	7.3
Calculated concentration (nM)	435	54.0	56.3	148	0.7